Yaw Moment Observer Design for Electric Vehicles Considering Vehicle Speed Variation

Yafei Wang, Hiroshi Fujimoto
Department of Advanced Energy, Graduate School of Frontier Science,
The University of Tokyo

Transdisciplinary Bldg. 7H1, 5-1-5 Kashiwanoha,
Kashiwa, Chiba, 277-8561 JAPAN
Phone: (81) 04-7136-3881
Fax: (81) 04-7136-3881
E-mail: wang@hori.k.u-tokyo.ac.jp, fujimoto@k.u-tokyo.ac.jp

Direct yaw-moment control (DYC) has long being considered as an effective control technology for vehicle stabilization in critical driving conditions and has been commercialized for modern vehicles. Different from internal-combustion-engine-based vehicles, the yaw moment input of electric vehicles (EVs) with in-wheel-motors can be realized in a more effective way for DYC: left and right wheels can be independently commanded and torque responses of motors are much faster than hydraulic brakes. In [1], a yaw moment observer (YMO) was designed, and it was demonstrated to be effective in yaw motion control of EVs. However, speed variation, which influences vehicle dynamics, was not addressed in the conventional YMO design. That is, the nominal plant of the conventional YMO is time-invariant which cannot represent speed-dependent characteristics of the vehicle; in fact, such control system may have to sacrifice stability margin. In this paper, a time-varying YMO is developed by considering changes of vehicle speed, and it gives improved performance compared with the conventional YMO.

Topics / Active safety and driver assistance systems

1. INTRODUCTION

Direct Yaw-moment Control (DYC) has been widely employed in modern vehicles to enhance stability and controllability. For traditional vehicles, differential braking between left and right wheels is usually employed to generate required yaw moment for lateral motion control [2]. In case of electric vehicles (EVs) with in-wheel-motors (IWMs), as the torques of left and right wheels can be independently commanded and torque response of the motors are fast, the required yaw moment for DYC can be realized in an more effective way [3]. In [4], a desired yaw rate model was derived, and DYC was applied to a small single-seat EV driven by IWMs; the proposed control system was evaluated by both simulations and experiments. Considering that body slip angle is one of the key enablers for DYC control, [5] proposed a body slip angle estimation method and applied it to DYC control of an EV. Based on the principle of disturbance observer (DOB), [1] proposed a yaw moment observer (YMO)-based DYC, in which vehicle speed-related terms are treated as disturbances and the nominal model becomes a first order system with constant dynamic behavior. As this method is very practical, it was utilized in many EV control applications [6]-[7]. However, depending on longitudinal vehicle speed, vehicle dynamics varies; neglecting this fact may limit the performances of the DYC system. Therefore, in this paper, a gain-scheduled YMO is developed by considering changes of vehicle speed, i.e., the YMO parameters are speed-dependent and the nominalized plant can keep speed-related characteristics of the vehicle. Therefore, the dynamics of an EV can be treated specifically at any given vehicle speed. The remainder of this paper is arranged as: in Section 2, lateral vehicle model and conventional YMO is briefly reviewed; in Section 3, the proposed speed-dependent YMO is explained and stability analysis are provided; to show the improved control performance compared with conventional YMO, simulations and experiments are demonstrated in Section 4; conclusions and future works are given in Section 5.

2. REVIEW OF CONVENTIONAL YAW MOMENT OBSERVER

The lateral dynamics of an EV with two rear IWMs is illustrated in Fig. 1, and the governing equation is given in Eq. 1, where β and γ are the body slip angle and the yaw rate at the vehicle's center of gravity (CoG), respectively, δ_f is the front-steering angle, V_x and V_y are the vehicle's longitudinal and lateral velocities, respectively, V_{cg} is the vehicle's velocity at CoG, I is the moment of inertia about the yaw axis, C_f and C_r are the

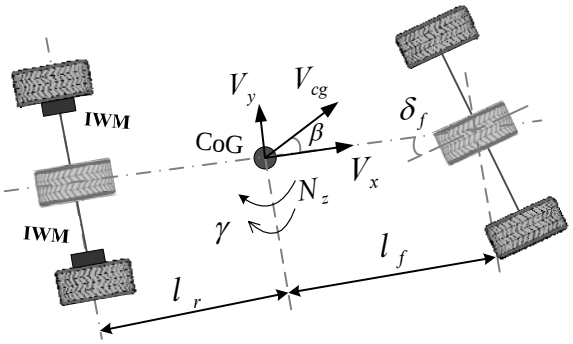

Fig. 1. Model of lateral motion for an EV with two rear IWMs.

cornering stiffness of the front and rear wheels, respectively, l_f and l_r are the distances from the CoG to respectively, N_z is the yaw moment generated by the differential torque of the rear wheels, which is used as control input in this research, and N_d is the disturbance-induced yaw moment.

$$I \cdot \dot{\gamma} = 2 \cdot l_f \cdot C_f(\delta_f - \frac{l_f}{V_x}\gamma - \beta) - 2 \cdot l_r \cdot C_r(\beta - \frac{l_r}{V_x}\gamma) + N_z + N_d \quad (1)$$

The yaw moment generated by lateral forces is defined as

$$N_t = 2 \cdot l_f \cdot C_f(\delta_f - \frac{l_f}{V_x}\gamma - \beta) - 2 \cdot l_r \cdot C_r(\beta - \frac{l_r}{V_x}\gamma) \quad (2)$$

and the total disturbance yaw moment is defined as $N_{dt} = N_t + N_d$. Then, Eq. 1 can be simplified as

$$I \cdot \dot{\gamma} = N_z + N_{dt} \quad (3)$$

In [1], YMO is designed by nominalizing Eq. 3 as Eq. 4. Obviously, the nominal system is independent of vehicle speed.

$$\gamma = \frac{1}{I_n \cdot s} \cdot N_{in} \quad (4)$$

In Fig. 2 (a), the concept of conventional YMO is illustrated, and in Fig. 2 (b), the yaw rate reference can be obtained using

$$\gamma^* = \frac{k(V_x)}{\tau \cdot s + 1} \cdot \delta_f \quad (5)$$

where k is a gain that should be tuned based on V_x. Although the reference is time varying, the nominalized plant cannot reflect the characteristics of a real vehicle because it is time invariant. In Section 3, this issue will be further analyzed in terms of stability margin. Furthermore, it can be seen from the lower figure of Fig. 2 that such a controller consists of a two-degree-of-freedom controller and a YMO, and yaw rate is used as feedback signal. It was demonstrated that this is an effective approach for yaw motion stabilization [6]-[7].

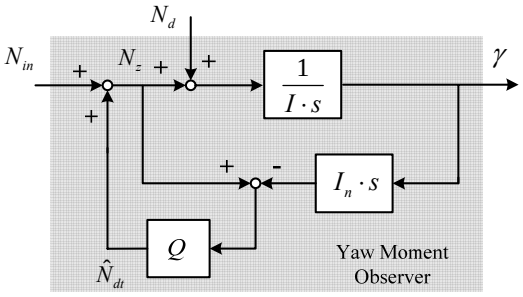

(a) Yaw moment observer.

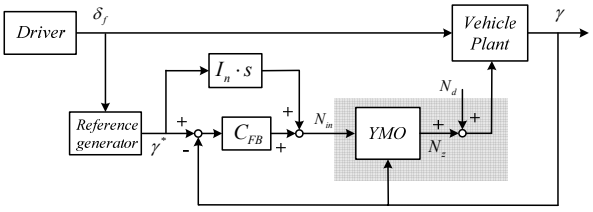

(b) YMO-based yaw motion control system.

Fig. 2 Illustration of YMO and YMO-based yaw controller.

3. GAIN-SCHEDUALED YAW MOMENT OBSERVER FOR DIRECT YAW CONTROL

Speed-dependent YMO Design. From Eq. 1, it can be seen that V_x is associated with yaw rate terms. Therefore, by moving all the γ-related terms to the left side, Eq. 1 can be rearranged as

$$I_n \cdot \dot{\gamma} + 2 \cdot \frac{C_f \cdot l_f^2 + C_r \cdot l_f^2}{V_x} \cdot \gamma = 2 \cdot l_f \cdot C_f(\delta_f - \beta) - 2 \cdot l_r \cdot C_r \cdot \beta + N_z + N_d \quad (6)$$

In a similar manner to the design of conventional YMO, Eq. 6 can be simplified as

$$I_n \cdot \dot{\gamma} + 2 \cdot \frac{C_f \cdot l_f^2 + C_r \cdot l_f^2}{V_x} \cdot \gamma = N_z + N_{td} \quad (7)$$

and then, Eq. 7 is nominalized as

$$P_n = \frac{\gamma}{N_{in}} = \frac{1}{\left(I_n \cdot s + 2 \cdot \frac{C_{f,n} \cdot l_{f,n}^2 + C_{r,n} \cdot l_{f,n}^2}{V_x} \right)} := \frac{1}{\left(I_n \cdot s + \frac{\alpha_n}{V_x} \right)} \quad (8)$$

and the block diagram of the proposed YMO and the overall control system for yaw motion stabilization are illustrated as Fig. 3 (the blocks for γ^* generation is neglected).

Stability Margin. Next, the stability margins of conventional and proposed YMO will be compared. First, the transfer function (vehicle plant) from yaw moment input to yaw rate can be given as Eq. 9.

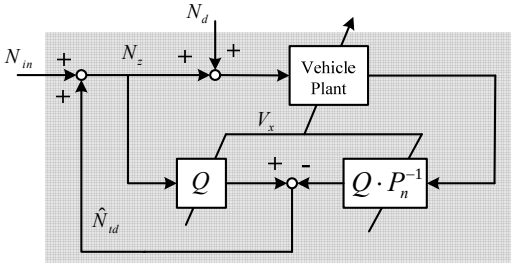

(a) Speed-dependent yaw moment observer.

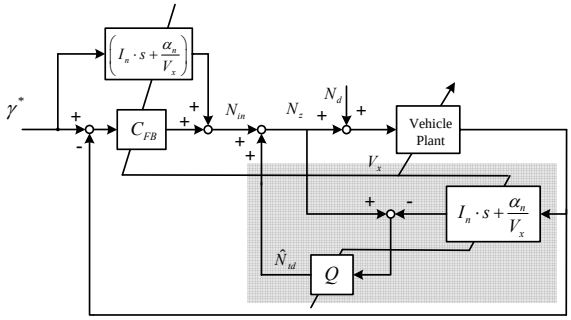

(b) Speed-dependent YMO-based yaw motion control system.

Fig. 3 Illustration of gain-scheduled YMO and DYC controller.

$$P_{N_z}^{\gamma}(s) = \frac{\gamma(s)}{N_z(s)} = G_{N_z}^{\gamma}(0) \cdot \frac{T_{\gamma N_z} \cdot s + 1}{\frac{s^2}{\omega_n^2} + \frac{2 \cdot \xi \cdot s}{\omega_n} + 1} \quad (9)$$

where

$$\omega_n = \frac{2 \cdot l}{V_x} \cdot \sqrt{\frac{C_f \cdot C_r}{m \cdot I}\left(1 + A V_x^2\right)},$$

$$A = -\frac{m}{2 \cdot l^2} \cdot \frac{l_f \cdot C_f - l_r \cdot C_r}{C_f \cdot C_r},$$

$$\xi = \frac{m \cdot \left(l_f^2 \cdot C_f + l_r^2 \cdot C_r\right) + I \cdot \left(C_f + C_r\right)}{2 \cdot l \cdot \sqrt{m \cdot I \cdot C_f \cdot C_r \cdot \left(1 + A V_x^2\right)}},$$

$$T_{\gamma N_z} = \frac{m \cdot V_x}{2 \cdot \left(C_f + C_r\right)},$$

$$G_{N_z}^{\gamma}(0) = \frac{V_x \cdot \left(C_f + C_r\right)}{2 \cdot C_f \cdot C_r \cdot l^2 \cdot \left(1 + A \cdot V_x^2\right)}.$$

and the equivalent representation of YMO and feedback controller can be given as

$$K_{eq} = \frac{C_{FB} + Q \cdot P_n^{-1}}{1 - Q} \quad (10)$$

where Q is selected to be a first order low pass filter and C_{FB} is the feedback controller. In the comparison, C_{FB} is designed by using pole placement method based on the normalized models, and the open loop stability margins are compared in Table 1 (vehicle speed is assumed to be varying from 5-80 kph).

Table 1. Stability margin comparison.

	Phase margin [deg]
Conventional YMO	14.3-49.8 (5-80 kph)
Proposed YMO	89.1-97 (5-80 kph)

From Table 1, it can be observed that: 1) the phase stability margin of the proposed method is larger than that of the conventional YMO, 2) the range of the phase stability margin of the proposed YMO is narrower in comparison with that of the conventional method. That is, the proposed method gives more stable performance than the conventional one.

Q Filter Design. Normally, the Q can be selected to be a first order or second order filter [7]. In this part, a method for second-order Q-filter design is introduced (note that in the simulations and experiments, the Q is set as a first order low pass filter for fair comparison, and this part only provides an illustrative way for Q filter design). From Eq. 7, the system can be represented in a state space form as

$$\begin{aligned} \dot{x} &= A \cdot x + B \cdot u \\ y &= C \cdot x \end{aligned} \quad (11)$$

where

$$A = \begin{bmatrix} \frac{-\alpha_n}{I_n \cdot V_x} & \frac{1}{I_n} \\ 0 & 0 \end{bmatrix}, \quad B = \begin{bmatrix} \frac{1}{I_n} \\ 0 \end{bmatrix},$$

$$C = \begin{bmatrix} 1 & 0 \end{bmatrix}, \quad x = \begin{bmatrix} \gamma \\ N_{td} \end{bmatrix}, \quad u = N_z.$$

Therefore, the state can be estimated as Eq. 12, where $\hat{y} = C \cdot \hat{x}$, and K is the observer gain.

$$\dot{\hat{x}} = A \cdot \hat{x} + B \cdot u + K \cdot \left(y - \hat{y}\right) \quad (12)$$

Eq. 12 can then be transformed as

$$\begin{aligned} \dot{\hat{x}} &= \left(A - K \cdot C\right) \cdot \hat{x} + B \cdot u + K \cdot y \\ &:= \overline{A} \cdot \hat{x} + B \cdot u + K \cdot y \end{aligned} \quad (13)$$

and $\hat{x}$ is obtained as

$$\hat{x} = \left(s \cdot I - \overline{A}\right)^{-1} \cdot B \cdot u + \left(s \cdot I - \overline{A}\right)^{-1} \cdot K \cdot y \quad (14)$$

and then, the disturbance can be obtained as Eq. 15, where $C_d = [0 \quad 1]$.

$$\begin{aligned} \hat{N}_{td} = C_d \cdot \hat{x} = C_d \cdot \left(s \cdot I - \overline{A}\right)^{-1} \cdot B \cdot u + \\ C_d \cdot \left(s \cdot I - \overline{A}\right)^{-1} \cdot K \cdot y \end{aligned} \quad (15)$$

The above equation can be represented as Fig. 4. By comparing Fig. 3 (a) with Fig. 4, it can be observed that

$$Q = -C_d \cdot \left(s \cdot I - \overline{A}\right)^{-1} \cdot B \quad (16)$$

Assume K is given as $\begin{bmatrix} K_1 & K_2 \end{bmatrix}^T$, Q can then be

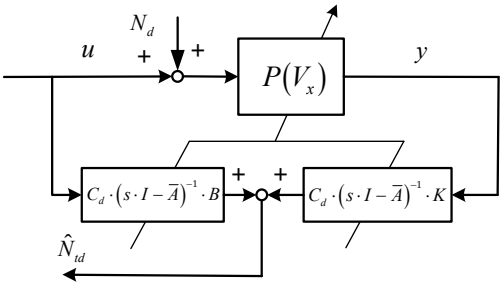

Fig. 4 Alternative representation of the gain-scheduled YMO.

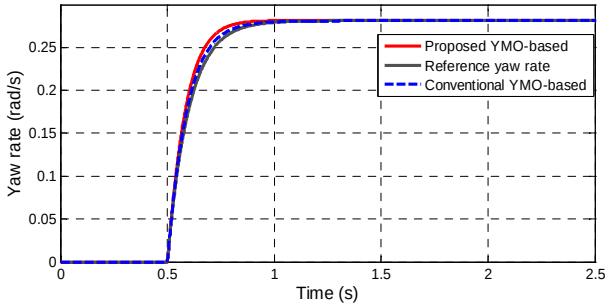

Fig.5 Simulation comparison of the proposed and conventional YMOs (constant speed).

designed as a second order filter:

$$Q = \frac{K_2}{I_n \cdot s^2 + \left(K_1 \cdot I_n + \frac{\alpha_n}{V_x} \right) \cdot s + K_2} \qquad (17)$$

4. SIMULATIONS AND EXPERIMENTS

Simulations. Based on the parameters of our experimental EV "Kanon", simulations were conducted to verify the proposed method, and the specification of the EV is provided in the Appendix.

First of all, the situation when the EV runs at a constant speed of 50 km/h is considered, and the vehicle is assumed to be given a step steering of 0.07 rad from 0.5 second to avoid an obstacle. A reference yaw rate is generated using the model defined in Section 2, and both the conventional and the proposed methods were simulated to check the reference tracking performance. For fair comparison, the feedback controllers were set to be the same, and the results are shown in Fig. 5. As can be seen, both of the two methods can track reference yaw rate very well, and no big difference can be observed between them.

However, DYC is usually activated in critical driving conditions in reality. That is, the driver may accelerate or decelerate the vehicle by mistake or intentionally, and steers the vehicle to avoid an obstacle at the same time. Based on this scenario, simulations were conducted to compare the proposed gain-scheduled YMO with the conventional YMO. Again, a step steering of 0.07 rad from 0.5 second was applied. Moreover, to simulate real situations, cornering

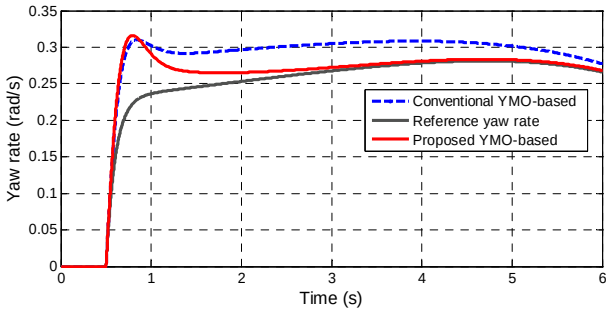

(a) Deceleration case.

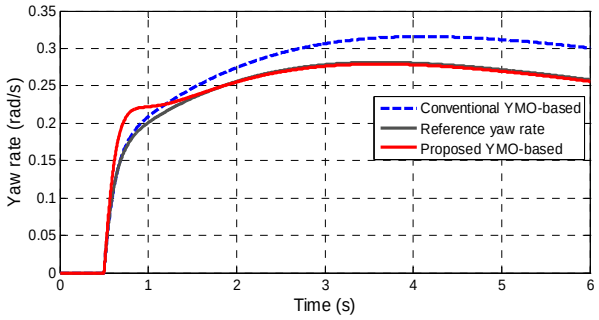

(b) Acceleration case.

Fig.6 Simulation comparison of the proposed and conventional YMOs (varying speed).

stiffness of the real plant and the nominalized plant were set differently. In Fig. 6 (a), the vehicle is assumed to decelerate from 100 km/h to 35 km/h with a deceleration rate of 3 m/s^2, and in Fig. 6 (b), the vehicle is assumed to accelerate from 10 kph to 75 kph with an acceleration rate of 3 m/s^2. Two points can be observed: 1) the reference yaw rates vary due to the varying of speed; 2) although the conventional YMO cannot provide satisfying tracking performance, the proposed YMO can control the vehicle to track the desired yaw rate very well.

Experiments. Using the experimental EV "Kanon", preliminary experiments were conducted to verify the proposed controller. Specifically, low friction sheets were set up in the test field to let the EV generates large enough lateral motion for clearer demonstration, and the test field photo is shown in the Appendix.

The scenario for the experiments is very similar to a fishhook test: the EV first accelerates in front of an area of low friction road, and then decelerates when the vehicle run into the low friction area, a step steering input is given by the driver to generate large lateral force. At this step, as steering is handled by the driver, steering angles could not be exactly the same; therefore, yaw rates without control, with conventional YMO control and with proposed YMO control are plotted separately in Figs. 7, 8 and 9; the speed pattern are also provided. Obviously, both the conventional YMO control and with proposed YMO control can suppress excessive yaw motion, and the proposed speed-dependent YMO gives better performance compared with the conventional method.

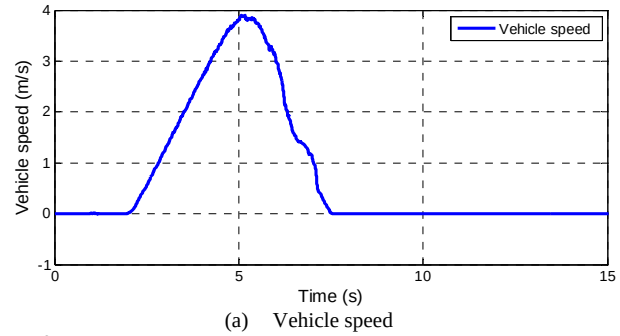

(a) Vehicle speed

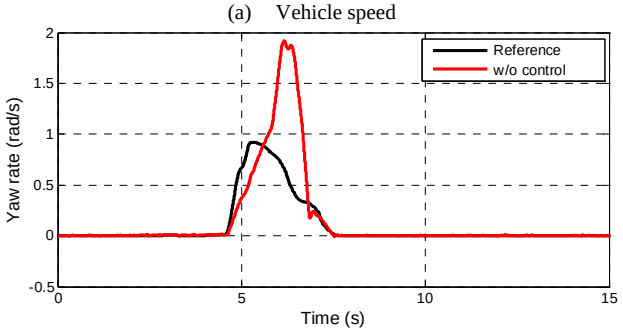

(b) Yaw rate

Fig.7 Experimental result (w/o control).

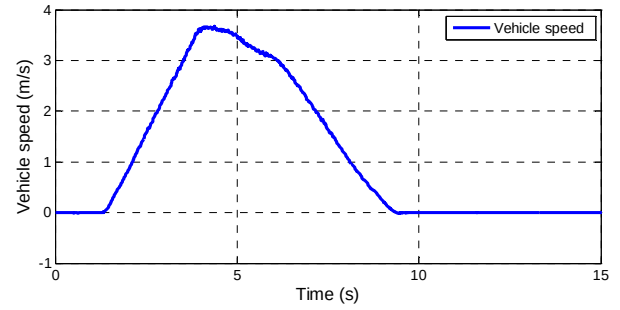

(a) Vehicle speed

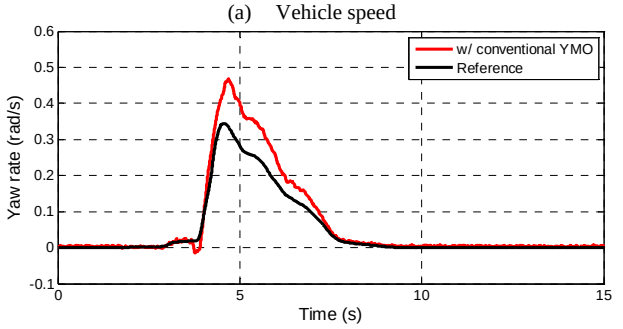

(b) Yaw rate

Fig.8 Experimental result (w/o conventional YMO).

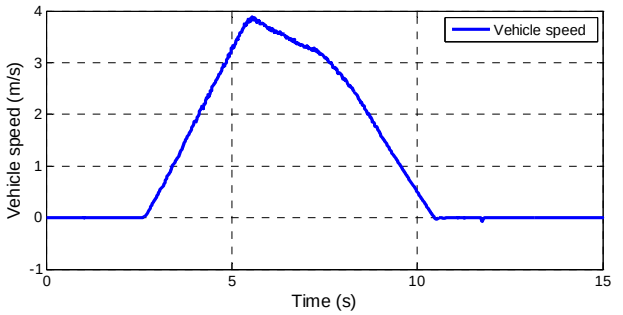

(a) Vehicle speed

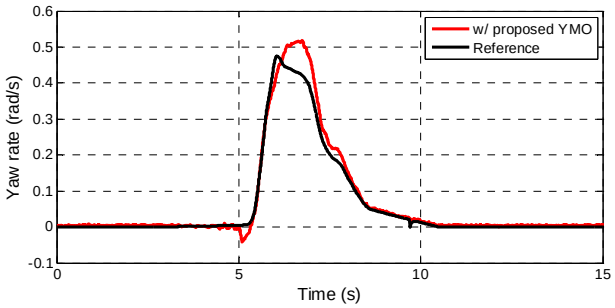

(b) Yaw rate

Fig.9 Experimental result (w/o proposed YMO).

5. CONCLUSION AND FUTURE WORKS

In this paper, aimed at improving control performance, a speed-dependent YMO design method is proposed and is verified using simulations and experiments. Future works involve: 1) to provide the same yaw rate reference for comparison, a step steering pattern using EPS will be utilized; 2) systematic design of feedback controller and YMO will be studied.

APPENDIX

Table 2. Vehicle specification.

	Description	Value
M	vehicle mass	850 kg
l_f	distance from CoG to front axle	1.013 m
l_r	distance from CoG to rear axle	0.702 m
C_f	cornering stiffness of front wheel	1.013 m
C_r	cornering stiffness of rear wheel	0.702 m
I	vehicle yaw moment of inertia	617 kg·m^2

(a) Experimental vehicle

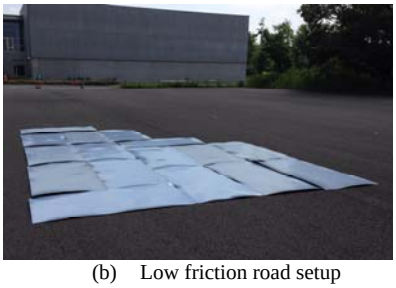

(b) Low friction road setup

Fig.10 Experimental vehicle and test field.

The specification of the EV considered in this research in given in Table 2, and the photos for the EV and test field are shown in Fig. 10.

REFERENCES

[1] H. Fujimoto, T. Saito, and T. Noguchi, “Motion stabilization control of electric vehicle under snowy conditions based on yaw-moment observer,” Proc. of 8th IEEE International Workshop on Advanced Motion Control, 2004, pp.35-40.

[2] E. Esmailzadeh, A. Goodarzi, and G. R. Vossoughi “Optimal yaw moment control law for improved vehicle handling,” Int. J. Mechatronics, vol. 13, no. 7, pp.659-675, 2003

[3] Y. Hori, “Future vehicle driven by electricity and control-research on four-wheel-motored “UOT Electric March II”,” IEEE Trans. Ind. Electron., vol.51, no.5, pp.954-962, 2004.

[4] P. Raksincharoensak, M. Shino, and M. Nagai, “Investigation of Intelligent Driving Assistance System by Using Direct Yaw Moment Control,” Review of Automotive Engineering, vol.25 no.2, pp.185-192, 2004.

[5] C. Geng, L. Mostefai, M. Denai, and Y. Hori, “Direct Yaw-Moment Control of an In-Wheel-Motored Electric Vehicle Based on Body Slip Angle Fuzzy Observer,” IEEE Trans. Ind. Electron., no.5, pp.1411-1419, 2009.

[6] Y. Yamauchi, and H. Fujimoto, “Vehicle Motion Control Method Using Yaw-moment Observer and Lateral Force Observer for Electric Vehicle,” IEEJ Transactions on Industry Applications, vol.130, no .8; pp.939-944, 2010.

[7] K. Maeda, H. Fujimoto, and Y. Hori, “Fundamental study on design method of Yaw-Moment Observer for improvement of drivers' comfort for electric vehicle,” in Proc. of 37th Annual Conference on IEEE Industrial Electronics Society, pp.3846-3851, 2011.